Chemical Physics Letters 593 (2014) 72–76

Contents lists available at ScienceDirect

Chemical Physics Letters

journal homepage: www.elsevier.com/locate/cplett

The absorption spectrum of C_{60} in *n*-hexane solution revisited: Fitted experiment and TDDFT/PCM calculations

E. Menéndez-Proupin [a,b,*], Alain Delgado [c,d], Ana L. Montero-Alejo [a,e], J.M. García de la Vega [a]

[a] Departamento de Química Física Aplicada, Facultad de Ciencias, Universidad Autónoma de Madrid, 28049 Madrid, Spain
[b] Departamento de Física, Facultad de Ciencias, Universidad de Chile, Las Palmeras 3425, 780-0003 Ñuñoa, Santiago, Chile
[c] CNR-NANO S3 Center, Institute for Nanoscience, Via Campi 213/A, 41125 Modena, Italy
[d] Centro de Aplicaciones Tecnológicas y Desarrollo Nuclear (CEADEN), Calle 30 # 502, 11300 La Habana, Cuba
[e] Laboratorio de Química Computacional y Teórica, Facultad de Química, Universidad de la Habana, 10400 La Habana, Cuba

ARTICLE INFO

Article history:
Received 14 October 2013
In final form 28 December 2013
Available online 6 January 2014

ABSTRACT

The UV absorption spectrum of C_{60} in *n*-hexane solvent has been revised by means of numerical analysis and time-dependent density functional theory (TDDFT). The absorption spectrum in the range 3–7 eV has been fitted by a spectral function that includes fourteen transitions with Gaussian lineshape, providing reference transition energies and intensities. The agreement between the experimental and theoretical UV absorption intensities has been considerably improved with respect to previous calculations, by including the solvent dielectric response via the polarizable continuum model (PCM).

1. Introduction

The discovery of the fullerenes triggered a revolution in organic chemistry, fulfilling many of the predictions stated in the seminal article of Kroto et al. [1]. Nowadays, fullerenes are the building blocks of molecular complexes and extended solids with many potential applications in the fields of photovoltaics, hydrogen storage and nanomedicine [2–4] which has made them the object of study of thousands of articles since they were discovered.

As the wave of research has shifted from the prototypical C_{60} towards fullerene derivatives [5–8] with many interesting opto-electronic properties, the optical response of the basic unit remains still not fully understood. This is partially a consequence of the difficulty of matching the object of theoretical simulations (isolated and frozen C_{60}), with the experimental measurements performed either in hot gas phase [9,10] or embedded in a condensed medium [11–14]. The absolute values of the transition strength determined from gas spectra are inaccurate due to the large error (~200%) in determining the partial pressures [10]. Moreover, the integrated strengths of the bands are likely to be modified by highly excited vibrational states and by the temperature dependent population of the states. Due to these facts, the spectra for C_{60} in solution are believed to approximate better the spectrum of the isolated molecule at low temperature. On the other hand, the computation of the optical properties of the isolated C_{60} is difficult due to the large number of electrons and the fact that the infrared and visible range of the spectrum has no dipole-allowed excitation. In this region light absorption is mediated by vibronic modes, which makes very complex the interpretation and the calculations. In the UV range, the spectrum is dominated by dipole-allowed excitations and has not been well described by *ab initio* methods. This is the problem that we will address in this Letter.

The work of Leach et al. [11] on C_{60} in *n*-hexane solution provides the most detailed up to date quantitative characterization of the C_{60} UV–vis spectrum. The experimental results have been interpreted by doing calculations mainly for isolated molecules [15,16]. The complete neglect of differential overlap for spectroscopy (CNDO/S) [17] and time-dependent density functional theory (TDDFT) [18] have emerged as the most used theoretical methods. However, the theoretical and measured oscillator strengths (OSs) are quite different. The OSs for random orientations are defined as $f_i = \left(2m_e E_i/3\hbar^2 e^2\right)|\langle i|\mathbf{d}|0\rangle|^2$, where m_e is the electron mass, $\mathbf{d}$ is the dipole operator, and E_i is the energy of excitation from state 0 to *i*. CNDO/S calculations combined with the configuration interaction of single excitations (CIS) have predicted OSs one order of magnitude larger than those obtained in the experiments. This behavior is due to a reduced active space, as has been discussed in Ref. [19]. On the other hand, TDDFT calculations with large basis sets are reported to give OSs one order of magnitude smaller than the experimental OSs [16,20]. Xie et al. [20] have computed the first two dipole allowed transitions using TDDFT with several functionals, as well as time-dependent Hartree–Fock (TDHF) and semiempirical methods. They have used small basis sets, such as STO-3G and 3–21G. However, they show that their results are qualitatively consistent with the calculations with larger basis sets (e.g. Ref. [16]). The values of the excitation energies and OSs are similar

* Corresponding author at: Departamento de Física, Facultad de Ciencias, Universidad de Chile, Las Palmeras 3425, 780-0003 Ñuñoa, Santiago, Chile. Fax: +56 2 2271 2973.
E-mail address: emenendez@uchile.cl (E. Menéndez-Proupin).

0009-2614/$ - see front matter © 2014 Elsevier B.V. All rights reserved.
http://dx.doi.org/10.1016/j.cplett.2013.12.067

with all non-hybrid functionals, while hybrid functionals produce energies 1 eV in excess, and OSs about five and two times larger than non-hybrid functionals for the first and second excitation, respectively. This discrepancy is mitigated using the long-range corrected functional CAM-B3LYP [21]. TDHF produces excitation energies more than 2 eV higher than the experiment, a wrong pattern of OSs, and a negative triplet excitation energy. The problems of Hartree–Fock approximation for the ground state of C_{60} have been examined in Ref. [22]. Recently, Fukuda and Ehara [23] have calculated the UV spectrum using the *ab initio* cluster expansion method. Their results imply some changes in the interpretation of the spectrum.

A different set of OSs [24], which are about four times lower than the set given by Leach et al. [11], have been compared with the former experimental and theoretical values [20]. However, these OSs are defined by a different expression. They describe the dielectric function of an idealized solid of non-interacting C_{60} molecules, which in turn have been obtained by a numerical transformation of the spectrum in solution using the Maxwell–Garnett effective medium equation. Hence, there is no straightforward method to compare them with the standard OSs.

The spectrum is influenced by the dielectric response of the solvent, which modifies the transition energies and strengths. Several attempts have been made to extract the spectrum of the molecule from the solution measurements [13,25,26]. Some authors [13,25] have correlated the transition energies in a variety of solvents with the Lorentz–Lorenz polarizability parameter $P = (\epsilon - 1)/(\epsilon + 2)$, and extrapolated the energies to vacuum condition ($\epsilon = 1$). Andersen and Bonderup [26] have shown that deduction of the isolated cross section from solution spectra is possible only for isolated narrow lines. Otherwise, the real part of the polarizability need to be known. They have fitted the solution spectra using a model polarizability represented by a sum of Lorentzians. While they obtain sensible values for the OSs and transition energies, their fitted spectrum evidences that the inhomogeneous broadening and a few more transitions need to be considered.

In the present Letter, we present a least-squares fitting of the UV experimental spectrum [16]. On the other hand, we simulate directly the spectrum in *n*-hexane solution, considering the dielectric solvent effects within the TDDFT/PCM method.

2. Analysis of the experimental spectrum

The UV spectrum is dominated by three wide strong bands with maxima at 3.78, 4.84, and 5.88 eV. These peaks are labeled as *c, e* and *g* in Figrue 1, following the notation of Bauernschmitt et al. [16]. Also, at 3.04 and 3.07 eV there is a small double peak (labeled *a*) attributed to the first allowed transitions and a phonon replica. Between 3.17 and 3.40 eV there are several small shoulders that are attributed to vibron states associated with the first and second allowed transitions[11]. Other noticeable shoulders appear at higher energies, labeled as *d, f* and *h*. The assignment of the peaks, as well as some shoulders was guided by CNDO/S calculations. Leach et al. [11] estimated the OSs of the main electronic transitions from the band maxima and half-widths, assuming Gaussian band shapes. Table 1 displays detailed information on the optical transitions in the UV–vis spectrum, obtained from the analysis of the experiments and from calculations. The first columns show the assignment of dipole-allowed transitions made in Ref. [11]. The above procedure is inaccurate in presence of overlapping bands, and does not provide results for not so strong transitions that produce shoulders on the spectrum. To overcome this difficulty, we have obtained the OSs from least-squares fitting. We have fitted the UV spectrum using the nonlinear least-squares Marquardt–Levenberg algorithm as implemented in gnuplot[27]. We have

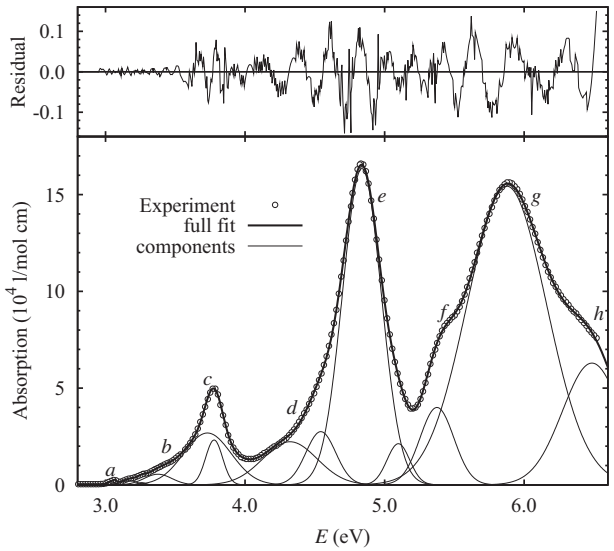

Figure 1. Experimental absorption spectrum by C_{60} in *n*-hexane solution (Ref. [16]), the fitting function, and their difference (residuals).

Table 1
Transition energies (E) and oscillator strengths (f) and bandwidths (σ), determined from experiments and computed with TDDFT in vacuum and in solvent with the C-PCM method. The units of E and σ are eV, f is dimensionless. The theoretical f of the triple degenerated states are added up.

	E;f Ref. [11]	E;f;σ Fit (this Letter)	E;f TDDFT ($\epsilon = 1$)	E;f TDDFT/PCM ($\epsilon = 1.8819$)
a_1	3.04; 0.015	3.04; 0.003; 0.03	2.870; 0.007	2.868; 0.013
a_2	3.07	3.07; 0.001; 0.01		
a_3		3.17; 0.010; 0.05		
b_1	3.30; –	3.26; 0.003; 0.03		
b_2		3.37; 0.047; 0.10		
c_1	3.78; 0.37	3.72; 0.398; 0.17	3.564; 0.420	3.534; 0.796
c_2		3.78; 0.123; 0.06		
d_1	4.06; –	4.31; 0.378; 0.19		
d_2	4.35; 0.10	4.54; 0.257; 0.11		
e_1	4.84; 2.27	4.83; 1.985; 0.14	4.546; 1.128	4.488; 2.090
e_2		5.10; 0.151; 0.08	5.043; 2×10^{-5}	5.041; 1×10^{-4}
f	5.46; 0.22	5.37; 0.424; 0.12	5.171; 0.007	5.163; 0.018
g	5.88; 3.09	5.86; 3.828; 0.28	5.545; 2.373	5.452; 4.101
			5.759; 0.071	5.755; 0.074
h	6.36; –	6.48; 1.160; 0.21	6.076; 2.379	6.007; 2.545

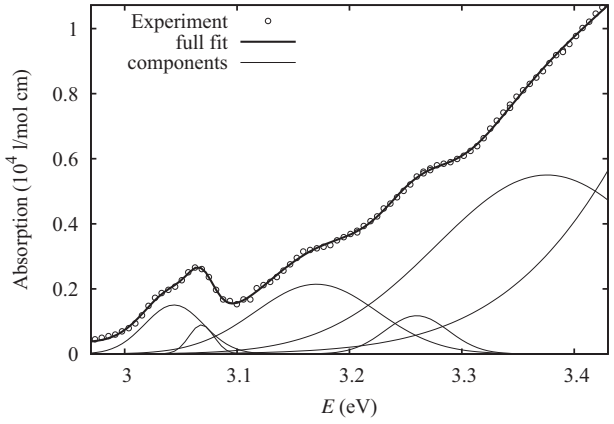

Figure 2. Low energy range experimental absorption spectrum and the fitting function.

taken the numerical values of the molar absorption coefficient (as defined in the Beer–Lambert law) from Figure 2 of Ref. [16]. The data was then fitted by the function

$$\epsilon(E) = \frac{\pi N_A e^2 h}{(\ln 10) m_e c} \sum_i \frac{E}{E_i} \frac{f_i}{\sqrt{2\pi\sigma_i^2}} \exp\left[-\frac{(E-E_i)^2}{2\sigma_i^2}\right], \quad (1)$$

where N_A, e, h, m_e, c are the Avogadro number, the electron charge, the Planck constant, the electron mass and the speed of light, respectively. The factor before the summation is equal to 2.87066×10^4eV l/(cm mol). The Gaussian function accounts for fluctuations of transition energies, and it is justified by the excellent fit achieved. We have obtained a very good fit with the parameters shown in Table 1.

The result can be appreciated in Figures 1 and 2, where the thick solid line shows the fitted curve, and the thin lines show the individual contributions. Two sets of parameters must be distinguished. One set (I) describes the transitions *a* and *b*, the OSs of which are very small and are believed to arise from one or two allowed transitions and vibron replicas (see Figure 2). The second set (II) describes the transitions at energies higher than 3.7 eV (labeled *c*–*h*), and have large OSs, and combine in three strong bands (see Figure 1). If the fitting process is performed varying all the parameters at the same time, some parameters of the set I can show the following behavior: (i) converge to unphysical values, such as negative OSs, (ii) two energies coalesce in one, or (iii) the shift out of range. However, they describe small peaks or shoulders that are observed consistently in the spectra [11,16,24,28]. When the Marquardt–Levenberg algorithm is applied in the range from 2.98 to 3.50 eV, varying the parameters of set I and keeping fixed the set II, the set I is stable and the root means square of the residuals is equal to 60 l/mol cm. However, the broadening and oscillator strengths present high statistical correlation and must not be considered accurate. The parameters of set II are more reliable, and were fitted in the range from 2.98 to 6.55 eV. The root mean square of the residuals in this range is 4.7×10^2 l/mol cm. There is still high correlation between the transitions at d_1 and d_2. This is not surprising because they rather describe a background of the strong bands. Leach et al. identified two transitions in this region, but assigned a joint oscillator strength of 0.10. There is also strong correlation between the OS of the transition c_2 and the width and strength of the transition c_1. However, both transitions are needed to describe the shape of this band, as well as to obtain a good fit of the set I.

Let us mention that our first intention was to fit only the bandwidths, keeping the energies and OSs with the values of Ref. [11]. In this case we obtained a poor fit. Fitting the OSs improved the fit, although allowing to vary also the energies was very important to obtain a good match between the experimental data and the model curve. This is due to the presence of broad features that do not correspond to computed electronic transitions and were disregarded in the analysis of Ref. [11]. The present fit is also better than the one presented by the authors in Ref. [19]. A similar least-squares fit has been performed for C_{60} in ice at 40 K [29]. These results are rather similar to ours in the transition energies. In this case, there are evident contributions equivalent to b_2, c_1, c_2, d_1, e_1, *f*, and *g*, and many more transitions at the red edge of the *b* band.

3. TDDFT calculations

We have performed TDDFT calculations of the C_{60} by using the General Atomic and Molecular Electronic Structure System (GAMESS) code[30]. Following Ref. [16], we have used the 6–31G basis set augmented by a diffuse *s*-function [31,32] and the XC functional BP86 [33,34]. This basis set seems to be sufficiently complete, as the computed spectrum is similar to that calculated with a plane waves scheme [35]. Figure S1 of Supplementary Material shows both Gaussian and plane waves calculations, and more arguments supporting the basis set employed. The first 350 singlet excited states have been computed in order to study the fullerene optical response in an interval ranging from 1.8 eV (695 nm) to 6.2 eV (202 nm). The structural model of C_{60} was taken from the fullerite crystal structure[36] and it was relaxed using DFT calculations in a supercell 20 Å in size (see Ref. [19] for details).

The calculated energies of C_{60} in vacuum, shown in Table 1, are almost equal to the results of Ref. [16]. The OSs of Ref. [16] are one third of the results of our calculation, and one order of magnitude smaller than the experimental values. The dipole-allowed states in C_{60} have T_{1u} symmetry and they group in trifold degenerate levels with equal OSs. We believe that the OSs reported in Ref. [16] correspond to the individual states that form the triple level. In Table 1, we show the added strengths for each level, which is what must be compared with the experiments. With this correction, the OSs given by TDDFT calculations have the same order of magnitude as in the experiment. However, the theoretical OSs are still systematically lower than the experimental ones.

Better accuracy can be achieved, in principle, using long-range corrected functionals like CAM-B3LYP. Such calculation has been performed recently[21], and the strong dipole-allowed transitions have been obtained at energies 4.25, 4.62, and 5.56 eV. The corresponding oscillator strengths are 0.75, 0.33, and 1.93. These values are rather similar to our calculations (Table 1), the second and third energies being almost equal, as well as the OS order of magnitude. The main differences are in the first transition energy (0.7 eV higher with CAM-B3LYP) and the second transition OS, which is much lower with CAM-B3LYP, underestimating the experimental OS. Figure S2 of Supplementary Material shows these values in comparison to the experimental data and other calculations.

The *n*-hexane solvent acts upon C_{60} like a dielectric medium with dielectric constant $\epsilon = 1.8819$ at optical frequencies. The solvent effects have been accounted for in both, the ground and excited states calculations by using the conductor-like polarizable continuum model (C-PCM) [37] as implemented in GAMESS. In the framework of PCM the solvent is represented as a structureless infinite continuum characterized by its dielectric constant. In our calculations the solute–solvent interactions are limited to those of electrostatic origin. That is, the interaction of the fullerene with the reaction field is due to the solvent polarization. The results can be appreciated in Table 1. On the other hand, the OSs of the absorption lines are enhanced by the presence of solvent, improving the agreement with the values fitted from the experiment. The OSs need a further correction due to the fact that the electric field acting upon the C_{60} molecules is different from the macroscopic field of the electromagnetic wave. In the classical Onsager model, the local and the macroscopic fields are related by the expression [26] $\mathbf{E}_{loc} = [G/(1-R\alpha)]\mathbf{E}$, where $G = 3\epsilon/(2\epsilon+1)$ is a factor accounting for the enhancement of the field in a spherical cavity and $1/(1-R\alpha)$ is a factor related to the reaction of the dielectric matrix due to the polarization of the medium by the dipole field of the molecule. The latest effect is included in the PCM formalism and does not need further correction. As the oscillator strength contains the square of the interaction matrix element, it is enhanced by a factor G^2. An additional factor $1/\sqrt{\epsilon}$ affects the absorption coefficient due to the change of the light velocity in the medium with respect to vacuum [26] (notice that $\sqrt{\epsilon}$ is the refraction index). Hence, the OS given by the C-PCM method have been multiplied by $G^2/\sqrt{\epsilon} = 1.024$ in Table 1.

4. Discussion

A crucial issue is how to match the excitations determined from fitting the spectrum and from the calculations. This question must

be solved before evaluating the performance of different theoretical methods for C_{60}. The peaks c, e and g have obvious theoretical excitations. Transitions a_1 and a_2 are reasonably matched with the first dipole allowed transition and a phonon replica. a_3 and other transitions identified [11], albeit too weak to be fitted, may also be phonon replicas of the same transition a_1 or other non-allowed excitation that are activated by vibrational motion or by the fluctuations of the environment. The same origin is possible for features b and d, noticing that d_1 and d_2 present large OSs. The f shoulder has been assigned a transition to a $5T_{1u}$ state [16]. However, this assignment is doubtful because the experimental OS is one order of magnitude larger than the theoretical one. As h is in the edge of the measured spectrum its parameters cannot be determined accurately and its OS is highly correlated with the parameters of peak g. Nonetheless, the TDDFT and TDDFT/PCM calculations predict a strong transition in this position that is twice as strong as that obtained in the experiment.

The most interesting assignment is that of c_1 and c_2, for which there is only one theoretical level. The closeness of both transition energies induce to assume that c_1 and c_2 correspond to the same excited level of the computed isolated frozen molecule. The fact that fitting this peak needs two Gaussians indicates that the fluctuations of the excitation energy are not completely random. As regards to e_2, and possibly d_2, their energy difference with e_1 induces to assume that they are associated with different transitions. The values of the OSs may help the assignment. The OS $f_{c_1} = 1.985$ is smaller than the value 2.27 given in Ref. [11]. If the OS is determined from the maximum and bandwidth of the e peak of our scanned data, we obtain 2.38 in nice agreement with Ref. [11]. Hence, the transition e_1 accounts for 83% of the apparent OS strength of the band. However, the added OSs of d_2, e_1 and e_2 equals 2.39, i.e, the apparent OS. The OS given by TDDFT is 1.128, a value rather lower than either f_{e_1} or the total band OS. The TDDFT/PCM OS is 2.090, in close correspondence with f_{e_1}. For the g peak, the fitted OS value of 3.828 is better approached by the TDDFT/PCM calculation, while the calculation without solvent clearly underestimate the experimental OS. For the a feature, the TDDFT calculation agrees better than TDDFT/PCM. However, if the OS of a_1, a_2 and a_3 are added, then the PCM result is better. The TDDFT OS for c transitions is close to the fitted value for c_1. On the other hand, the sum of f_{c_1} and f_{c_2} agrees with the general trend of being underestimated by TDDFT and overestimated by TDDFT/PCM. Hence, although we cannot be conclusive, we think that c_1 and c_2 are due to the same theoretical transition, while e_1 and g are the other two theoretical transitions.

The above picture is slightly changed by the calculations of Ref. [23], that were based on the symmetry adapted cluster-configuration interaction (SAC-CI) method. These calculations suggest that the a peak is due to vibronic interaction with a non-allowed excitation that has symmetry T_{2u}. The transition energies and OSs are shown in Figure S2 of the Supplementary Material. The first allowed transition, at 3.69 eV, would match the b band, with OS of 0.2, and the c peak would be due to the second allowed transition with OS of 1.265, with computed energy of 3.90 eV. The third allowed transition would have OS of 10.388 and matches the e peak. These oversized OSs and energies may be due to insufficient size of the active space, as it is the case with semiempirical calculations[19]. Moreover, it does not solve the splitting of c_1 and c_2, the existence of d_1 and d_2, and the high OS of f.

The lack of a theoretical line that can be matched with the experimental transition f at 5.37 eV deserves more discussion. TDDFT/PCM predicts transitions at 5.163 eV with an OS = 0.018, smaller than the experimental OS by a factor 1/23. CAM-B3LYP and SAC-CI calculations also fail to predict a comparable transition. Fluctuations in the solvent may activate silent modes, but one can hardly believe that the effect of fluctuations is big enough to cause such a large OS. Other possibilities are a defect in the molecule, or a charge-transfer absorption with participations of n-hexane molecules or a solvated impurity. It could also be a transition in charged C_{60} or even a complex manifestation of the Jahn–Teller effect. Further study is needed to clarify this issue, considering explicitly solvent molecules. Our results make clear that this study is necessary, because even with PCM, without explicit solvent molecules, the number of transitions is smaller in theory than in experiment.

Malaspina et al. [38] have performed molecular dynamics simulations of C_{60} in ethanol, and computed UV–vis spectra by doing semi empirical quantum calculations. Regretfully, the computed UV–vis spectrum are not shown. It is mentioned the obtention of a solvatochromic redshift, consistently with our PCM calculations. Other interesting property is the enhancement of the breathing vibrational mode of C_{60} due to coupling with the solvent. A breathing mode with high amplitude could modify differently optically active excited states, and explain the number of transitions not accounted for in the optical spectrum. An extension of that work to the case of n-hexane solvent is a natural step to elucidate the C_{60} UV–vis spectrum.

5. Conclusions

We have performed a numerical fit of the UV absorption spectrum of C_{60} in n-hexane solution. Our fit provides an analytical representation of the spectrum as a sum of fourteen Gaussian-type functions, with root mean square deviations of 4.7×10^2 l/mol cm in the range 2.98–6.55 eV. This function describes all the major features observed in the spectrum, as well as the most significant features in the range 2.98–3.4 eV. The fit has been analyzed in the light of a quantum chemistry calculation in the framework of TDDFT, including the solvent dielectric effects with the PCM approach. We show that the theoretical OSs are remarkably improved by the use of the solvent model.

Acknowledgements

This Letter was supported by the Grants SB2010–0119 (Ministry of Education), CTQ2010–19232 (MICIN), D/030752/10 and A1/035856/11 (AECID), and the FP7 Marie Curie IIF project HY-SUNLIGHT: 252906. A.D. acknowledges support by the European Communitys FP7 through the CRONOS project, Grant Agreement No. 280879.

Appendix A. Supplementary data

Supplementary data associated with this article can be found, in the online version, at http://dx.doi.org/10.1016/j.cplett.2013.12.067.

References

[1] H.W. Kroto, J.R. Health, S.C. O'Brien, R.F. Curl, R.E. Smalley, Nature 318 (1985) 162.
[2] T.M. Clarke, J.R. Durrant, Chem. Rev. 110 (2010) 6736.
[3] P. Chawla, V. Chawla, R. Maheshwari, S.A. Saraf, S.K. Saraf, Mini Rev. Med. Chem. 10 (2010) 662.
[4] D.V. Schur et al., Int. J. Hydrogen Energy 36 (2011) 1143.
[5] F. D'Souza, S. Gadde, M.E. Zandler, K. Arkady, M.E. El-Khouly, M. Fujitsuka, O. Ito, J. Phys. Chem. A 106 (51) (2002) 12393.
[6] G. Yang, Y. Si, Z. Su, J. Phys. Chem. A 115 (46) (2011) 13356.
[7] R. Zalesny et al., Phys. Chem. Chem. Phys. 12 (2010) 373.
[8] I.D. Petsalakis, D. Tzeli, I.S.K. Kerkines, G. Theodorakopoulos, Comp. Theor. Chem. 965 (2011) 168.
[9] Q. Gong, Y. Sun, Z. Huang, X. Zhou, Z. Gu, D. Qiang, J. Phys. B At. Mol. Opt. Phys. 29 (1996) 4981.
[10] A.L. Smith, J. Phys. B At. Mol. Opt. Phys. 29 (1996) 4975.
[11] S. Leach et al., Chem. Phys. 160 (1992) 451.

[12] D.J. van den Heuvel, I.Y. Chan, E.J.J. Groenen, J. Schmidt, G. Meijer, Chem. Phys. Lett. 231 (1994) 111.
[13] A. Sassara, G. Zerza, M. Chergui, S. Leach, Astrophys. J. Suppl. Ser. 135 (2001) 263.
[14] J. Catalán, P. Pérez, Fullerenes Nanotubes Carbon Nanostr. 10 (2002) 171.
[15] G. Orlandi, F. Negri, Photochem. Photobiol. Sci. 1 (2002) 289.
[16] R. Bauernschmitt, R. Ahlrichs, F.H. Hennrich, M.M. Kappes, J. Am. Chem. Soc. 120 (1998) 5052.
[17] J. del Bene, H.H. Jaffe, J. Chem. Phys. 48 (1968) 1807.
[18] M.A. Marques, C.A. Ullrich, F. Nogueira, A. Rubio, K. Burke, E.K.U. Gross (Eds.), Time-Dependent Density Functional Theory, Lecture Notes in Physics, Vol. 706, Springer, Berlin Heidelberg, 2006.
[19] A.L. Montero-Alejo, E. Menéndez-Proupin, M.E. Fuentes, A. Delgado, F.-P. Montforts, L.A. Montero-Cabrera, J.M. García de la Vega, Phys. Chem. Chem. Phys. 14 (2012) 13058.
[20] R.-H. Xie et al., J. Chem. Phys. 120 (2004) 5133.
[21] T. Fahleson, J. Kauczor, P. Norman, S. Coriani, Mol. Phys. 111 (2013) 1401.
[22] D. Stück, T.A. Baker, P. Zimmerman, W. Kurlancheek, M. Head-Gordon, J. Chem. Phys. 135 (2011) 194396.
[23] R. Fukuda, M. Ehara, J. Chem. Phys. 137 (2012) 134304.
[24] J. Hora, P. Pánek, K. Navrátil, B. Handlířová, J. Humlíček, Phys. Rev. B 54 (1996) 5106.
[25] J. Catalán, Chem. Phys. Lett. 223 (1994) 159.
[26] J.U. Andersen, E. Bonderup, Eur. Phys. J. D 11 (2000) 435.
[27] T. Williams et al., Gnuplot 4.2: an interactive plotting program, `http://gnuplot.sourceforge.net/` (September 2008)
[28] V.S. Pavlovich, E.M. Shpilevsky, J. Appl. Spectrosc. 77 (2010) 335.
[29] S.H. Cuylle, H. Linnartz, J.D. Throwers, Chem. Phys. Lett. 550 (2012) 79.
[30] M.W. Schmidt et al., J. Comput. Chem. 14 (1993) 1347–1363. a complete list of the authors that has contributed to GAMESS is found at the top of every log file from a GAMESS run. The program website is http://www.msg.ameslab.gov/gamess.
[31] D. Feller, J. Comp. Chem. 17 (1996) 1571.
[32] K.L. Schuchardt et al., J. Chem. Inf. Model. 47 (2007) 1045.
[33] A. Becke, Phys. Rev. A 38 (1988) 3098.
[34] J. Perdew, Phys. Rev. B 33 (1986) 8822.
[35] D. Rocca, R. Gebauer, Y. Saad, S. Baroni, J. Chem. Phys. 128 (2008) 154105.
[36] D.L. Dorset, M.P. McCourt, Acta Crystallogr. Sect. A 50 (1994) 344.
[37] M. Cossi, V. Barone, J. Chem. Phys. 115 (2001) 4708.
[38] T. Malaspina, E.E. Fileti, R. Rivelino, J. Phys. Chem. B 111 (2007) 11935.